

3D Brain Tumor Segmentation Using Fuzzy Classification and Deformable Models

Hassan Khotanlou¹, Jamal Atif¹, Olivier Colliot², and Isabelle Bloch¹

¹ GET - Ecole Nationale Supérieure des Télécommunications, Dept TSI,
CNRS UMR 5141, 46 rue Barrault, 75634 Paris Cedex 13, France

² McConnell Brain Imaging Center, MNI, McGill University,
3801 University, Montréal, Québec, H3A2B4, Canada

{Hassan.Khotanlou, Jamal.Atif, Isabelle.Bloch}@enst.fr,
colliot@bic.mni.mcgill.ca

Abstract. A new method that automatically detects and segments brain tumors in 3D MR images is presented. An initial detection is performed by a fuzzy possibilistic clustering technique and morphological operations, while a deformable model is used to achieve a precise segmentation. This method has been successfully applied on five 3D images with tumors of different sizes and different locations, showing that the combination of region-based and contour-based methods improves the segmentation of brain tumors.

1 Introduction

Brain tumor segmentation from MR images is a challenging task that involves various disciplines including medicine, MRI physic, radiologist's perception, and image analysis based on intensity and shape. The literature is rich with techniques for segmenting normal brain structures, but many of these methods fail in the presence of a pathology. Actually the techniques that are intended for tumors leave significant room for increased automation, applicability and accuracy. In brain tumor studies, existence of abnormal tissues is most of the time easy to detect but accurate and reproducible segmentation and characterization of abnormalities still remain a challenging task.

Let us briefly summarize existing work, classically divided into region-based and contour-based methods. In the first class, a tumor segmentation method using knowledge based and fuzzy techniques was proposed by Clark et al. [2]. This method has two drawbacks. First, it requires multichannel images such as T1, T2 and PD. Furthermore a training phase prior to segmenting a set of images is necessary. Other methods are based on statistical pattern recognition techniques. Kaus et al. [6] have proposed a method for automatic segmentation of small brain tumors using a statistical classification method and atlas registration. Moon et al. [9] have also used the EM algorithm and atlas prior information for automatic tumor segmentation. These methods fail in the case of large deformations in the brain and they also require multichannel images (T1, T2, PD and contrast enhanced images) for classification. Prastawa et al. [12]

consider the tumor as an outlier and use a statistical classification for rough segmentation and then geometric and spatial constraints for final segmentation. The fuzzy connectedness method was proposed by Moonis et al. [10] for tumor segmentation. In this semi-automatic method, the user must select the region of the tumor. The calculation of connectedness is achieved in this region and the tumor is delineated in 3D as a fuzzy connected object containing the seed points of the tumor that were selected by the user. Other methods such as data fusion [1], atlas based [4] and transformation [13] methods have been developed, with similar drawbacks.

In contour-based methods, Lefohn et al. [7] have proposed a semi-automatic method for tumor segmentation by level sets. The user selects the tumor region and after the deformation process, he adapts the level set parameters. Zhu and Yang [15] introduce an algorithm using neural networks and a deformable model. Their method processes each slice separately and is not a real 3D method. Ho et al. [5] have proposed level set evolution with region competition for tumor segmentation. Their algorithm uses two images (T1-weighted with and without contrast agents) and calculates a tumor probability map using classification, histogram analysis and the difference between the two images, and then this map is used as the zero level of the level set evolution. The deformable methods suffer from the difficulty of determining the initial contour, and tuning the parameters.

In this paper we propose a fully-automatic method that is a combination of region-based and contour-based methods. It does not require any user supervision, works in 3D and on standard routine T1 acquisitions. It combines a fuzzy classification method (FPCM) [11], morphological operations and a parametric deformable model, thus taking advantages of both approaches while cancelling their drawbacks. The method is detailed in Section 2, and results are presented in Section 3.

2 Tumor Segmentation Procedure

A preliminary stage consists of brain segmentation. For this purpose, a robust method using histogram scale-space analysis and morphological operations [8] is applied. This method first calculates statistical parameters of the main classes of tissues, which will be used in the classification procedure. After extracting the brain, the histogram based Fuzzy Possibilistic C-Mean method is used for rough segmentation of the tumor. This rough segmentation is used as the initial surface of a deformable model for the final precise tumor segmentation.

2.1 Classification Using FPCM and Morphological Operations

Fuzzy Possibilistic c-Means was introduced by Pal et al. [11] for classification. It is a combination of Fuzzy c-Means and Possibilistic c-Means algorithms. In data classification, both membership and typicality are mandatory for data structures interpretation. FPCM computes these two factors simultaneously. FPCM solves the noise sensitivity defect of FCM and also overcomes the problem of coincident clusters of PCM. The objective function of FPCM is:

$$J_{m,\eta}(U, T, V; X) = \sum_{i=1}^c \sum_{k=1}^n (u_{ik}^m + t_{ik}^\eta) \|X_k - V_i\|^2 \tag{1}$$

where $m > 1$, $\eta < 1$, $0 \leq u_{ik} \leq 1$, $0 \leq t_{ik} \leq 1$, $\sum_{i=1}^c u_{ik} = 1$, $\forall k$, $\sum_{k=1}^n t_{ik} = 1$, $\forall i$, X_k denotes the characteristics of a point to be classified (here we use grey levels), V_i is the class center, c the number of classes, n the number of points to be classified, u_{ik} the membership of point X_k to class i , and t_{ik} is the possibilistic typicality value of X_k associated with class i .

In order to detect and label the tumor we use a histogram based FPCM that is faster than the classical FPCM implementation. Since the process of the brain extraction provides an estimation of the cerebro spinal fluid (CSF), white matter (WM) and gray matter (GM) radiometric characteristics, we exploit this information to overcome the classical initialization problem, i.e. the algorithm is initialized with class centers which are very close to the final ones. We classify the extracted brain into five classes, CSF, WM, GM, tumor and background (at this study stage we do not consider the edema). To obtain the initial value of the class centers, we use the results of histogram analysis in the extraction step. We have used the mean of the CSF, WM and GM (\mathbf{m}_G , \mathbf{m}_W and \mathbf{m}_C) (calculated in brain extraction step) as the centers of their classes. For background, the value zero is used. To select the tumor class we assume that the tumor has the highest intensity among the five classes (this is the case in our study where we are interested in hyper-intensity pathologies such as full-enhancing tumors).

Several binary morphological operations (opening, erosion, largest component selection, etc.) are then applied to the tumor region in order to correct misclassification errors. The results of this step for two images are shown in Figure 1.

2.2 Refinement Using a 3D Deformable Model

To obtain an accurate segmentation, a parametric deformable method, that has been applied successfully in our previous work to segment internal brain structures [3], is used. The segmentation obtained from the previous processing is transformed into a triangulation using an isosurface algorithm based on tetrahedra and is decimated and converted into a simplex mesh \mathbf{X} . The evolution of the deformable surface \mathbf{X} is described by the following dynamic force equation:

$$\gamma \frac{\partial \mathbf{X}}{\partial t} = \mathbf{F}_{int}(\mathbf{X}) + \mathbf{F}_{ext}(\mathbf{X}) \tag{2}$$

where \mathbf{F}_{int} is the internal force that specifies the regularity of the surface and \mathbf{F}_{ext} is the external force that drives the surface towards image edges. The chosen internal force is:

$$\mathbf{F}_{int} = \alpha \nabla^2 \mathbf{X} - \beta \nabla^2 (\nabla^2 \mathbf{X}) \tag{3}$$

where α and β respectively control the surface tension (prevent it from stretching) and rigidity (prevent it from bending) and ∇^2 is the Laplacian operator. It

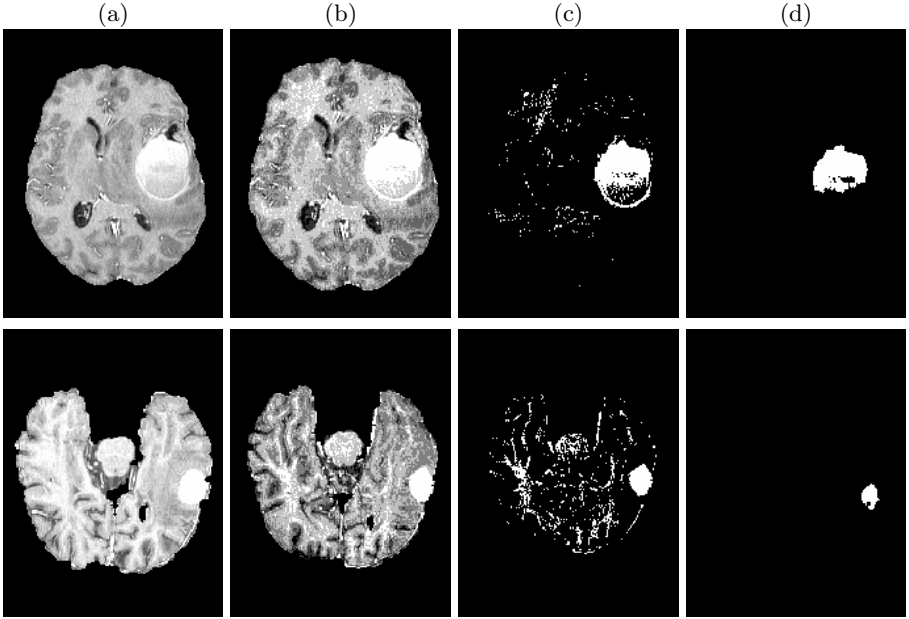


Fig. 1. Results obtained in the classification step for two 3D images. (a) One axial slice of extracted brain. (b) Result of FPCM classification. (c) Result of the thresholding. (d) Result after morphological operations.

is then discretized on the simplex mesh using the finite difference method [14]. In our case, the external force is derived from image edges. It can be written as:

$$\mathbf{F}_{ext} = v(x, y, z) \quad (4)$$

where v is a Generalized Gradient Vector Flow (GGVF) field introduced by Xu et al. [14]. A GGVF field v is computed by diffusion of gradient vector of a given edge map and is defined as the equilibrium solution of the following diffusion equation:

$$\frac{\partial v}{\partial t} = g(\|\nabla f\|)\nabla^2 v - h(\|\nabla f\|)(v - \nabla f) \quad (5)$$

$$v(x, y, z, 0) = \nabla f(x, y, z) \quad (6)$$

where f is an edge map and the functions g and h are weighting functions which can be chosen as follows:

$$\begin{cases} g(r) = e^{-\frac{r^2}{\kappa}} \\ h(r) = 1 - g(r) \end{cases} \quad (7)$$

To compute the edge map, a linear spatial filtering which is usually associated to Canny-Deriche edge detector is applied. Our experience shows that the GGVF is not sensitive to parameter k and we set it to $k = 0.05$ for all cases. The parameters involved in \mathbf{F}_{int} were set to $\alpha = 0.25$ and $\beta = 0.0$. Again the same parameters were used for all tests.

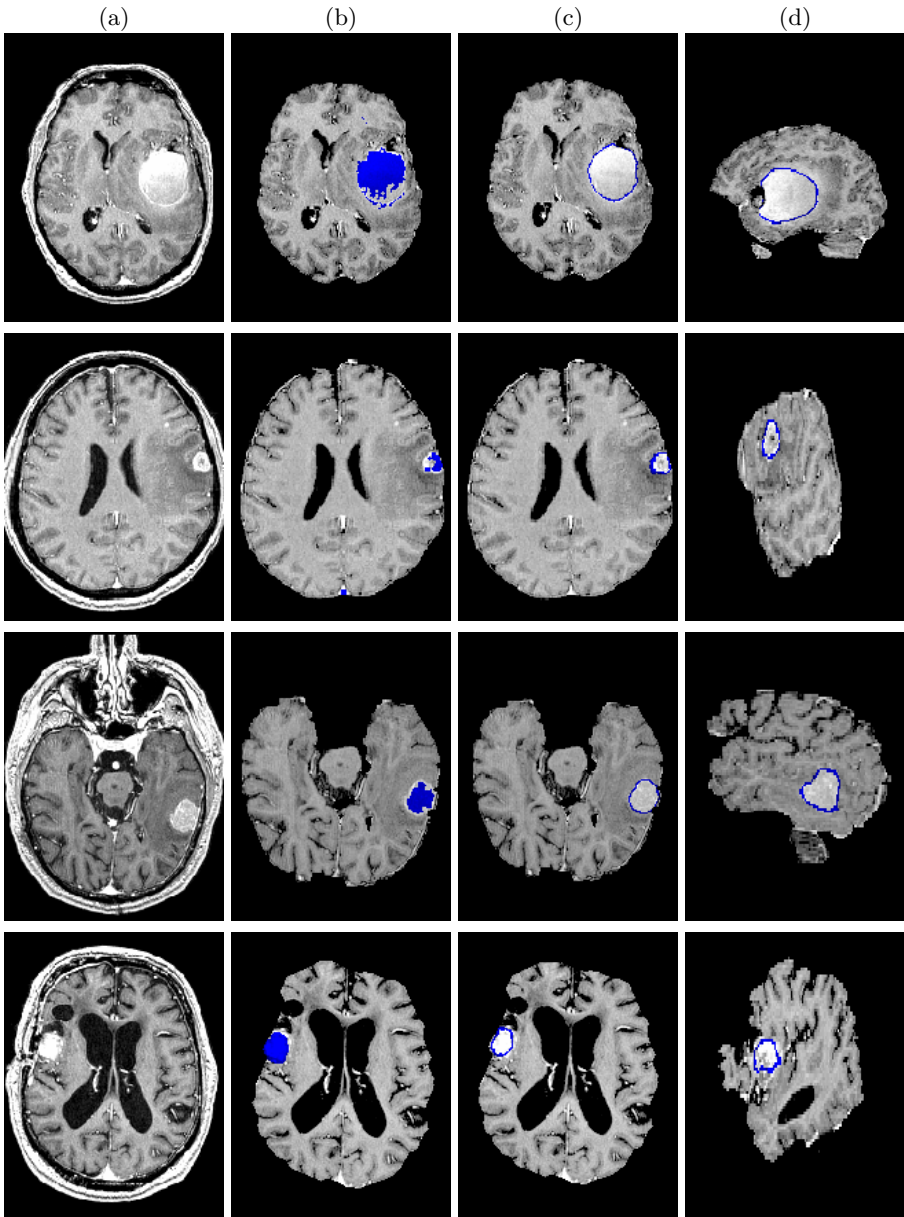


Fig. 2. Results obtained on four 3D images (obtained with the same parameters). (a) One axial slice of the original 3D image. (b) Result of the extracted brain and classification. (c) Final contour, superimposed on the axial slice. (d) Final contour, superimposed on a sagittal slice.

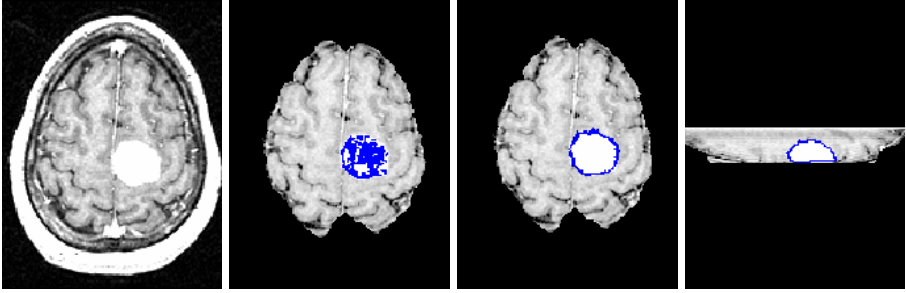


Fig. 3. Results obtained on one 3D image ($256 \times 256 \times 22$ voxels and obtained with the same parameters). (a) One axial slice of the original 3D image. (b) Result of the extracted brain and classification. (c) Final contour, superimposed on the axial slice. (d) Final contour, superimposed on a sagittal slice.

3 Results and Conclusion

We applied our algorithm to five different real 3D T1-weighted MR images ($256 \times 256 \times 124$ voxels and $256 \times 256 \times 22$ voxels). They exhibit tumors with different sizes and at different locations. We obtained good results for the five datasets without changing any parameter. The segmentation results of five datasets are shown in Figures 2 and 3.

We developed a hybrid algorithm using contour-based and region-based methods to segment brain tumors in 3D MR images. It exploits the advantages of fuzzy classification for automating the algorithm and the good quality segmentation result of deformable models to improve the segmentation. This is achieved by combining the FPCM classification method, morphological operations and a parametric 3D deformable model. Application on several datasets with different tumor sizes and different locations shows that this method works automatically with high quality of segmentation, and is robust to inter-individual variability for the all types of fully enhancing tumors. More tests are however necessary to further validate the approach. For quantitative evaluation of the results of segmentation, unfortunately there are not any standard images or methods. One way consists in comparing the results with manual segmentations. We are preparing these images for further evaluations with the help of medical experts.

Future work aims at assessing spatial relations to other structures around the tumor. Also we are extending this method for detecting several tumors in the brain and segmenting the edema.

Acknowledgments. We would like to thank Professor Desgeorges at Val-de-Grâce hospital for providing the images and his medical expertise. The image used in Figure 3 was provided by the Center for Morphometric Analysis at Massachusetts General Hospital and is available at <http://www.cma.mgh.harvard.edu/ibsr/>.

References

1. A.S Capelle, O.Colot, and C. Fernandez-Maloigne. Evidential segmentation scheme of multi-echo MR images for the detection of brain tumors using neighborhood information. *Information Fusion*, 5:203–216, 2004.
2. M.C. Clark, L.O. Lawrence, D.B. Golgof, R. Velthuisen, F.R. Murtagh, and M.S. Silbiger. Automatic tumor segmentation using knowledge-based techniques. *IEEE Transaction on Medical Imaging*, 17(2), April 1998.
3. O. Colliot, O. Camara, R. Dewynter, and I. Bloch. Description of brain internal structures by means of spatial relations for MR image segmentation. In *The International Society of Optical Engineering. SPIE 2004 Medical Imaging*, volume 5370, pages 444–455, 2004.
4. M.B. Cuadra, C. Pollo, A. Bardera, O. Cuisenaire, J. Villemure, and J. Thiran. Atlas-based segmentation of pathological MR brain images using a model of lesion growth. *IEEE Transactions on Medical Imaging*, 23(10):1301–1313, October 2004.
5. S. Ho, E. Bullitt, and G. Gerig. Level set evolution with region competition: Automatic 3D segmentation of brain tumors. In *International Conference on Pattern Recognition*, pages 532–535, 2002.
6. M.R. Kaus, S.K. Warfield, A. Nabavi, E. Chatzidakis, P.M. Black, F.A. Jolesz, and R. Kikinis. Segmentation of meningiomas and low grade gliomas in MRI. In *International Conference on Medical Image Computing and Computer-Assisted Intervention (MICCAI)*, volume LNCS 1679, pages 1–10, 1999.
7. A. Lefohn, J. Cates, and R. Whitaker. Interactive, GPU-based level sets for 3d brain tumor segmentation. Technical report, University of Utah, April 2003.
8. J.-F. Mangin, O. Coulon, and V. Frouin. Robust brain segmentation using histogram scale-space analysis and mathematical morphology. In *International Conference on Medical Image Computing and Computer-Assisted Intervention (MICCAI)*, pages 1230–1241, 1998.
9. N. Moon, E. Bullitt, K.V. Leemput, and G. Gerig. Model-based brain and tumor segmentation. In *International Conference on Pattern Recognition*, volume 1, pages 526–531, 2002.
10. G. Moonis, J. Liu, J.K. Udupa, and D.B. Hackney. Estimation of tumor volume with fuzzy-connectedness segmentation of MR images. *American Journal of Neuroradiology*, 23:352–363, 2002.
11. N.R. Pal, K. Pal, and J.C Bezdek. A mixed c-mean clustering model. In *IEEE International Conference on Fuzzy Systems*, pages 11–21, 1997.
12. M. Prastawa, E. Bullitt, S. Ho, and G. Gerig. A brain tumor segmentation framework based on outlier detection. *Medical Image Analysis*, 18(3):217–231, 2004.
13. H. Soltanian-Zadeh, M. Kharrat, and P.J. Donald. Polynomial transformation for MRI feature extraction. In *SPIE*, volume 4322, pages 1151–1161, 2001.
14. C. Xu and J.L. Prince. Snakes, shapes and gradient vector flow. *IEEE transaction on Image Processing*, 7:359–369, 1998.
15. Y. Zhu and H. Yang. Computerized tumor boundary detection using a Hopfield neural network. *IEEE Transactions on Medical Imaging*, 16(1):55–67, 1997.